Interplay between parity-time symmetry, supersymmetry, and nonlinearity: An analytically tractable case example

Panayotis G. Kevrekidis*
Department of Mathematics and Statistics, University of Massachusetts, Amherst, Massachusetts 01003-4515, USA and Center for Nonlinear Studies and Theoretical Division, Los Alamos National Laboratory, Los Alamos, New Mexico 87545, USA

Jesús Cuevas–Maraver
Grupo de Física No Lineal, Departamento de Física Aplicada I, Universidad de Sevilla. Escuela Politécnica Superior, C/ Virgen de África, 7, 41011-Sevilla, Spain and Instituto de Matemáticas de la Universidad de Sevilla (IMUS). Edificio Celestino Mutis. Avda. Reina Mercedes s/n, 41012-Sevilla, Spain

Avadh Saxena
Center for Nonlinear Studies and Theoretical Division, Los Alamos National Laboratory, Los Alamos, New Mexico 87545, USA

Fred Cooper
Santa Fe Institute, Santa Fe, New Mexico 87501, USA and Center for Nonlinear Studies and Theoretical Division, Los Alamos National Laboratory, Los Alamos, New Mexico 87545, USA

Avinash Khare
Physics Department, Savitribai Phule Pune University, Pune 411007, India
(Received 12 July 2015; published 1 October 2015)

In the present work, we combine the notion of parity-time ($\mathcal{PT}$) symmetry with that of supersymmetry (SUSY) for a prototypical case example with a complex potential that is related by SUSY to the so-called Pöschl-Teller potential which is real. Not only are we able to identify and numerically confirm the eigenvalues of the relevant problem, but we also show that the corresponding nonlinear problem, in the presence of an arbitrary power-law nonlinearity, has an exact bright soliton solution that can be analytically identified and has intriguing stability properties, such as an oscillatory instability, which is absent for the corresponding solution of the regular nonlinear Schrödinger equation with arbitrary power-law nonlinearity. The spectral properties and dynamical implications of this instability are examined. We believe that these findings may pave the way toward initiating a fruitful interplay between the notions of $\mathcal{PT}$ symmetry, supersymmetric partner potentials, and nonlinear interactions.

DOI: 10.1103/PhysRevE.92.042901 PACS number(s): 05.45.Yv

I. INTRODUCTION

In the past 15 years, there has been tremendous growth in the number of studies of open systems bearing both gains and losses, motivated to a considerable degree by the study of the specially balanced parity-time ($\mathcal{PT}$)-symmetric dynamical models [1–3]. The original proposal of Bender and collaborators toward the study of such systems was made as an alternative to the postulate of Hermiticity in quantum mechanics. Yet, in the next decade, proposals aimed at the experimental realization of such $\mathcal{PT}$-symmetric systems found a natural "home" in the realm of optics [4,5]. Within the latter, the above theoretical proposal (due to the formal similarity of the Maxwell equations in the paraxial approximation and the Schrödinger equation) quickly led to a series of experiments [6]. In turn, these efforts motivated experiments in numerous other areas, which span, among others, the examination of $\mathcal{PT}$-symmetric electronic circuits [7,8], mechanical systems [9], and whispering-gallery microcavities [10].

In the same spirit, another important idea that was originally proposed in a different setting (namely that of high-energy physics [11]) but has recently found intriguing applications in the context of wave guiding and manipulation in the realm of optics is that of supersymmetry (SUSY) [12]. The main idea is that from a potential with desired properties, one can obtain a SUSY partner potential that will be isospectral to (i.e., possess the same spectrum as) the original one, with the possible exception of one eigenvalue. In fact, taking the idea one step further, starting from a desired ground-state eigenfunction, one can design the relevant supersymmetric partner potentials in a systematic fashion, as discussed, e.g., in [12], both for continuum and even for discrete problems. In fact, more recently, the two ideas (of $\mathcal{PT}$ symmetry, or anyway non-Hermiticity, and SUSY) have been combined to construct SUSY-partner complex optical potentials designed to have real spectra [13]. An expected application of these ideas that is now being explored (extending the spirit of corresponding studies in the $\mathcal{PT}$-symmetric setting [14]) is in using SUSY transformations to achieve transparent and one-way reflectionless complex optical potentials [15].

The above works have essentially constrained the interplay of $\mathcal{PT}$ symmetry and SUSY at the level of linear potentials. Naturally, however, except for very low optical intensity, the crystals considered in the relevant applications bear nonlinear features, e.g., due to the Kerr effect. Hence, our focus in the present work will be to extend these linear ideas of

*kevrekid@math.umass.edu

$\mathcal{PT}$ symmetry and SUSY to a nonlinear case example. Moreover, we will select an example that blends two additional characteristics. On the one hand, one of our supersymmetric partners will constitute a famous and well-known solvable model in quantum mechanics, namely, the celebrated Pöschl-Teller potential [16,17]. On the other hand, it will turn out to be the case that not only the linear but also the nonlinear variant of the problem will be analytically solvable, in fact for arbitrary powers of the nonlinearity, in a special limit and will naturally connect with the linear solutions of the potential. In what follows, in Sec. II we will first present the general theory of linear $\mathcal{PT}$-supersymmetric potentials. Then, in Sec. III we will consider the special nonlinear solutions and their asymptotic linear limit reduction. Numerical results will corroborate the above analytical findings and we will also explore the spectral and dynamical stability of the nonlinear waveforms. Finally, in Sec. IV, we will summarize our findings and present our conclusions.

As a clarification, it should be noted here that our aim is to explore the supersymmetric analog of a $\mathcal{PT}$-symmetric linear problem and then to consider the nonlinear extension of such a model, incorporating the cubic nonlinearity stemming from the Kerr effect; i.e., the supersymmetric partnership is only available in the linear case. One of the main benefits of such a consideration is that the supersymmetric partner of the linear problem (here, being the Pöschl-Teller potential) gives us the proper starting point for the emergence (the "bifurcation") of nonlinear states out of linear ones, since as the norm of the former tends to zero, the nonlinear problem solution converges to the linear problem solution.

II. LINEAR NON-HERMITIAN SUPERSYMMETRIC MODEL

As is done generally in the theory of SUSY, we consider an operator $\mathcal{A}$ such that

$$\mathcal{A} = \frac{d}{dx} + W, \tag{1}$$

where W is the superpotential and an operator $\mathcal{B}$ of the form

$$\mathcal{B} = -\frac{d}{dx} + W. \tag{2}$$

It is important to accentuate here (see also [13]) that in the case of a complex superpotential W, contrary to the Hermitian case of a real W, $\mathcal{B}$ is not a Hermitian adjoint operator of $\mathcal{A}$ (hence the different symbol). Then, defining the potentials $V^{(\pm)} = W^2 \mp W' + E$, with $V^{(+)} = V^{(-)} - 2W'$, we have that the operators

$$H^{(\pm)} = -\frac{d^2}{dx^2} + V^{(\pm)} \tag{3}$$

are isospectral, with the exception of the fundamental mode in the potential $V^{(+)}$ which lacks a counterpart in $V^{(-)}$. More specifically, the eigenvalues satisfy $E_n^{(+)} = E_{n-1}^{(-)}$ for $n \geqslant 1$ (see also [13]). We note in passing that the eigenvectors of the two cases are also related, i.e., $u_n^{(-)} = \mathcal{A}u_{n+1}^{(+)}$ and $u_{n+1}^{(+)} = \mathcal{B}u_n^{(-)}$.

Now, assuming that $W = f + ig$, $V^{(+)} = V_R^{(+)} + iV_I^{(+)}$, and $V^{(-)} = V_R^{(-)} + iV_I^{(-)}$, we find that (see [18]) the potentials have to satisfy the following conditions:

$$V_R^{(+)} = f^2 - g^2 - f', \tag{4}$$

$$V_I^{(+)} = 2fg - g', \tag{5}$$

$$V_R^{(-)} = f^2 - g^2 + f', \tag{6}$$

$$V_I^{(-)} = 2fg + g'. \tag{7}$$

The remarkable finding of the linear spectral analysis of [18] was that those authors, motivated by the sl(2,C) potential algebra were able to derive a number of special case examples of simple functional forms of complex W's which give rise to complex SUSY potentials. Arguably, one of the most remarkable of their examples concerns the superpotential

$$W(x) = \left(m - \tfrac{1}{2}\right)\tanh(x - c) - ib_I\,\mathrm{sech}(x - c), \tag{8}$$

which gives rise (assuming hereafter without loss of generality that $c = 0$) to the supersymmetric partners of the form

$$V^{(+)} = \left(-b_I^2 - m^2 + \tfrac{1}{4}\right)\mathrm{sech}^2(x) - 2imb_I\,\mathrm{sech}(x)\tanh(x), \tag{9}$$

$$V^{(-)} = \left(-b_I^2 - (m-1)^2 + \tfrac{1}{4}\right)\mathrm{sech}^2(x) - 2i(m-1)b_I\,\mathrm{sech}(x)\tanh(x). \tag{10}$$

We chiefly focus hereafter on the remarkable special case of $m = 1$, previously considered, e.g., in [19]. The exceptional characteristic of this case is that it stems from a real potential $V^{(-)}$ which is well known to be exactly solvable in the realm of elementary quantum mechanics, namely, the Pöschl-Teller potential [16,17]. While its eigenfunctions can also be written down in an explicit form by means of hypergeometric functions, here we will restrict our considerations to the relevant (bound state) eigenvalues which in the context of the above example assume an extremely simple form as

$$E_n^{(-)} = -\tfrac{1}{4}[2b_I - 2n - 1]^2. \tag{11}$$

Such bound-state eigenvalues only exist when $n < b_I - 1/2$. This, in turn, suggests that for the + superscript potential, it will be $E_n^{(+)} = E_{n-1}^{(-)}$, i.e., all the relevant bound-state eigenvalues should also emerge in the $\mathcal{PT}$-symmetric spectrum of the potential $V^{(+)}$, just as they appear in the Hermitian (real) spectrum of the potential $V^{(-)}$. The only eigenvalue that will not be captured by this relation is $E = -1/4$; see the relevant details on the spectrum of $V^{(+)}$ below. Furthermore, we expect that when varying b_I, bound-state eigenvalues will emerge as b_I crosses 0.5, 1.5, 2.5, ... in both the spectra of $V^{(\pm)}$.

All of these conclusions are fully corroborated by the results of Fig. 1. The spectrum of $H^{(+)}$ considered therein turns out to be real, as may be anticipated by the $\mathcal{PT}$ symmetry of the model, but more importantly, it turns out to be identical to that of its supersymmetric Pöschl-Teller partner, as can be

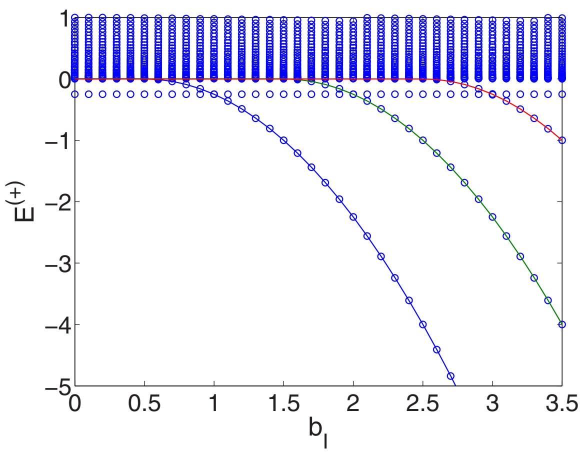

FIG. 1. (Color online) The blue circles represent the numerically computed eigenvalues $E^{(+)}$ of the operator $H^{(+)}$ of Eq. (3), under the $\mathcal{PT}$-symmetric potential of Eq. (9). The solid lines represent the analytical predictions based on the potential's supersymmetric partner $V^{(-)}$ corresponding to an analytically tractable Pöschl-Teller potential.

seen from the theoretical lines confirming the bifurcation of the point spectrum eigenvalues at the locations theoretically predicted. Finally, indeed, the only eigenvalue that is not captured is $E = -1/4$ which turns out to be *invariant*, under variations of b_I. We point out that generalizations of this potential with arbitrary coefficients in both the real and the imaginary parts were considered in [20] and the relevant $\mathcal{PT}$-symmetric transition threshold was identified as an inequality associating the real and the imaginary part prefactors. The pertinent inequality here assumes the form $(b_I - 1)^2 \geqslant 0$ and is generically satisfied (i.e., $\forall\ b_I$), as can be expected by the supersymmetric partnership of the potential with a Hermitian one bearing real eigenvalues for all b_I. It is also worthwhile to point out that the potential with functional dependences of the real and imaginary parts such as those of $V^{(+)}$ of Eq. (9) is also referred to as Scarff II potential [21–23].

As a side remark, we observe that $V^{(+)}$ is invariant under an exchange of b_I and m. Interestingly, as shown in [24], when $b_I - m$ is not an integer, the eigenvalue spectrum has two branches:

$$E_n^{(1)} = -(m - n - 1/2)^2\,, \quad n = 0,1,2,\dots,n_{\max}, \tag{12}$$

where $m - 3/2 \leqslant n_{\max} < m - 1/2$, and

$$E_n^{(2)} = -(b_I - n - 1/2)^2\,, \quad n = 0,1,2,\dots,n_{\max}, \tag{13}$$

where $b_I - 3/2 \leqslant n_{\max} < b_l - 1/2$.

From this, we infer that when $m = 1$ and b_I is not an integer, H^+ has two nodeless states (i.e., $n = 0$) with energy eigenvalues and eigenfunctions

$$E_0^{(1)} = -1/4, \quad \psi_0^{(1)} = \sqrt{\operatorname{sech}(x)}\, e^{2ib_I \tan^{-1}(\tanh x/2)}\,, \tag{14}$$

$$E_0^{(2)} = -(b_I - 1/2)^2, \quad \psi_0^{(2)} = \operatorname{sech}^{b_I - 1/2}(x)\, e^{2i \tan^{-1}(\tanh x/2)}\,, \tag{15}$$

although the latter (as per our spectral results of Fig. 1) will only be present for $b_I > 1/2$. Interestingly, while for $1/2 < b_l < 1$, $E_0 = -1/4$ is the ground state, for $1 < b_l < 3/2$, $E_0 = -(b_l - 1/2)^2$ corresponds to the ground state.

III. NONLINEAR GENERALIZATION OF THE MODEL

We now turn to the corresponding nonlinear model which is the basis for the present analysis. Examining the case of the focusing nonlinearity, the operator $H^{(+)}$ is augmented into the nonlinear problem:

$$iu_t = H^{(+)}u - |u|^{2\kappa}u. \tag{16}$$

The most physically relevant case is that of the cubic nonlinearity $\kappa = 1$, corresponding to the Kerr effect, although in recent years, examples of higher order nonlinearities (like $\kappa = 2$ and $\kappa = 3$) have been experimentally realized; for a recent example, see [25]. The relevant nonlinear problem has been partially considered for $\kappa = 1$ in a two-parameter generalization of the potential associated with $V^{(+)}$ [21]; see also the more recent discussions of [22,23]. While all of these works were restricted to the cubic case, below we will obtain exact solutions for arbitrary nonlinearity powers. Moreover, we will explain through our $\mathcal{PT}$-SUSY framework the existence of nonlinear dipole (and, by extension, tripole, etc.) solutions identified in [23], emerging from the higher excited states of the underlying linear problem. It can be directly found that the relevant nonlinear single-hump (nodeless) solution for arbitrary κ is of the form

$$u(x,t) = e^{-iEt} A \operatorname{sech}^{1/\kappa}(x) e^{i\phi(x)}, \tag{17}$$

where

$$A^{2\kappa} = \frac{4\kappa^2}{(\kappa+2)^2}\left[\frac{(\kappa+2)^2}{4\kappa^2} - 1\right]\left[\frac{(\kappa+2)^2}{4\kappa^2} - b_I^2\right], \tag{18}$$

$$\phi(x) = \frac{4\kappa b_I}{\kappa+2} \tan^{-1}\left[\tanh\left(\frac{x}{2}\right)\right], \tag{19}$$

and

$$E = -\frac{1}{\kappa^2}. \tag{20}$$

Note when $m = 0$ and $b_I = 1/2$, $V^{(+)} \to 0$ and our solution reduces to the well-known solution of the nonlinear Schrödinger (NLS) equation with $A^{2\kappa} = (1+\kappa)/\kappa^2$. Also note that when $\kappa = 2$, $A^{2k} \to 0\ \forall b_I$.

For $b_I \to b_{I,c}$, with $b_{I,c}^2 = \frac{(\kappa+2)^2}{4\kappa^2}$, the amplitude A tends to zero and the solution (17) becomes the solution of the corresponding linear limit (15) by virtue of condition (20). The solution (17) exists for $b_I < b_{I,c}$ when $\kappa < 2$ and for $b_I > b_{I,c}$ if $\kappa > 2$. Our analytical expression only yields the trivial solution for $\kappa = 2$ as mentioned earlier. Notice also that when b_I is fixed and κ varied, the solution tends to Eq. (14) when approaching the $\kappa = 2$ limit. Figure 2 shows the dependence of the norm with respect to b_I and κ when condition (20) for solution (17) is applied. The value of the norm is

$$N = \int_{-\infty}^{\infty} |u(x,t)|^2\, dx = A^2 B\left(\frac{1}{2}, \frac{1}{\kappa}\right), \tag{21}$$

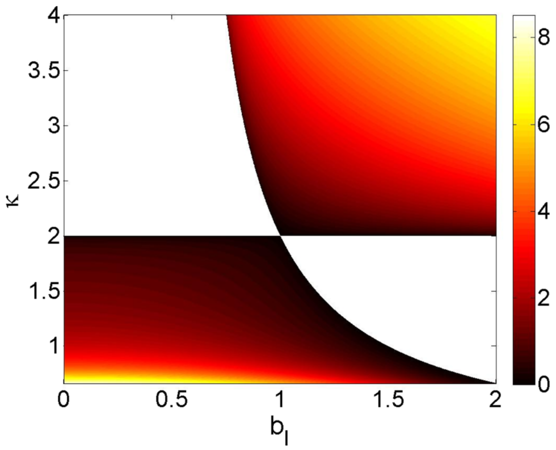

FIG. 2. (Color online) Norm of the solutions of Eq. (17) as a function of b_I and κ when $m = 1$.

where it has been taken into account that $A \in \mathbb{R}$ and $B(x,y)$ is Euler's beta function.

Horizontal "cuts" along the graph of Fig. 2 are shown in Figs. 3 and 4 where the continuum tendency to the linear limit (dark) is shown as a variation over b_I for $\kappa = 1$ and $\kappa = 3$, respectively. Apart from the analytical solution (17) which bifurcates from the nodeless solution of the linear Schrödinger equation, we have been able to find numerically the branch that bifurcates from the linear solution with a node [$n = 1$ in Eqs. (12) and (13)]. These solutions are the generalizations (for arbitrary κ) of the "dipoles" of [23]. In those cases, solutions exist as long as $b_I < b_{I,c} + 1$ and their monotonicity for $\kappa > 2$ is opposite to that of the fundamental solutions analytically identified above (hence, the above-mentioned

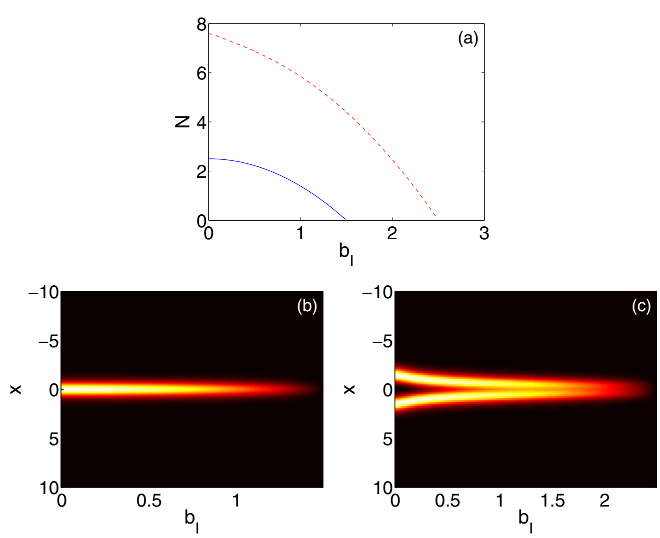

FIG. 3. (Color online) Panel (a): Norm of the solutions with $\kappa = 1$ as a function of b_I. The blue (full) line corresponds to the nodeless solution whereas the red (dashed) line corresponds to the "dipole" branch (see [23]) possessing a node. Panel (b) [(c)] showcases the modulus of the nodeless solution [solution with a node] as a function of x for different values of b_I. It can clearly be seen that the amplitude of the solution goes to 0 as $b_I \to 3/2$ [$b_I \to 5/2$].

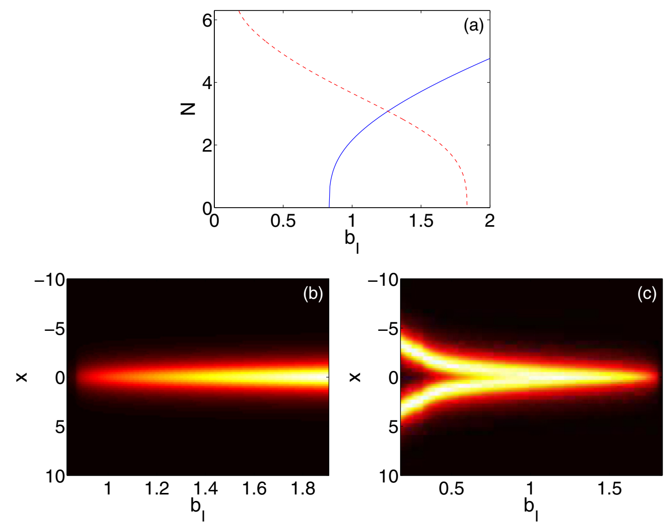

FIG. 4. (Color online) Panel (a): Norm of the solutions with $\kappa = 3$ as a function of b_I. The blue (full) line corresponds to the nodeless solution whereas the red (dashed) line corresponds to the solution with a node (i.e., the "dipole"). Panel (b) [(c)] showcases the modulus of the nodeless solution [solution with a node, although the node itself disappears as b_I increases] as a function of x for different values of b_I. It can clearly be seen that the amplitude of the solution goes to 0 as $b_I \to 5/6$ [$b_I \to 11/6$], i.e., the corresponding linear limit value for $E = -1/9$.

collision). Interestingly, it is worth mentioning that the latter dipole branch is present even for $\kappa = 2$. In the same spirit, higher order generalizations (e.g., tripoles, quadrupoles, etc.) can also be expected in the spirit of [23], degenerating to the linear limit, respectively, for $b_I \to b_{I,c} + 2$ and $b_I \to b_{I,c} + 3$, etc.

We now turn to the detailed stability analysis of the relevant soliton solutions (which was not explored systematically in [21,22], but was touched upon in [23] for $\kappa = 1$). In fact, in [21] a particular case example of an evolution (see Fig. 2 therein), as well as the positivity of the Poynting vector flux, led those authors to conclude that the relevant solutions were nonlinearly stable. However, our systematic spectral stability analysis, illustrated in Figs. 5 and 7, indicates otherwise. In particular, we use a linearization ansatz of the form

$$u(x,t) = e^{iEt}[u_0(x) + (a(x)e^{\lambda t} + b^{\star}(x)e^{\lambda^{\star} t})], \qquad (22)$$

where $u_0(x)$ is the spatial profile of the standing wave solution of Eq. (17), while $\{a(x), b(x)\}$ and λ correspond, respectively, to the eigenvector and eigenvalue of the linearization around the solution. The existence of eigenvalues with $\mathrm{Re}(\lambda) > 0$ would in this ($\mathcal{PT}$-symmetric and hence still ensuring the quartet symmetry of the relevant eigenvalues) context signals the presence of an instability.

We can see in Fig. 5 that indeed such an instability is present in the interval $0.56 < b_I < 1.37$ for the nodeless solutions of $\kappa = 1$. Further examination of the relevant phenomenology in Fig. 6 reveals the origin of the instability and its *stark* contrast with the corresponding phenomenology in the standard nonlinear Schrödinger (NLS) equation model. In particular, the breaking of translational invariance (due to the presence of the potential) leads the corresponding neutral

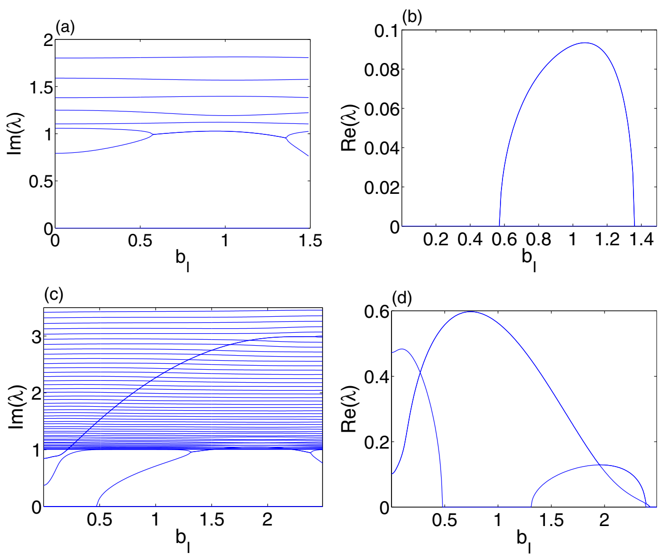

FIG. 5. (Color online) Imaginary part [panels (a) and (c)] and real part [panels (b) and (d)] of the eigenvalues associated with the linearization around the solution of the nodeless [(a) and (b)] and the single-node (i.e., dipole) solution branches [panels (c) and (d)] for $\kappa = 1$. It can be observed that the nodeless solutions become unstable in the interval $0.56 < b_I < 1.37$, whereas the solutions with a single node are unstable for all b_I except for a very small interval $2.43 < b_I < 2.5$ close to the upper existence limit; in addition, for $b_I < 0.48$ the latter waveform is also exponentially unstable.

mode to exit along the imaginary axis of the spectral plane (λ_r,λ_i) of the eigenvalues $\lambda = \lambda_r + i\lambda_i$. However, it is well known [26] that in the standard Hamiltonian case, the relevant "internal mode" of the solitary wave associated with translation has a positive energy or signature and hence its collisions with other modes, including ones of the continuous spectrum, do not lead to instability. Here, however, as illustrated in Fig. 6 exactly the opposite occurs. As the parameter b_I is varied, the relevant eigenvalue moves toward the continuous spectrum (whose lower limit is $\lambda = \pm i$) and the collision with it leads to a complex eigenvalue quartet, a feature that would never be possible for a single soliton of the regular NLS, under a translation-symmetry-breaking perturbation. This is a remarkable feature of the $\mathcal{PT}$-symmetric NLS model that is worthy of further exploration, possibly utilizing the notion (recently discussed for $\mathcal{PT}$-symmetric models in [27]) of Krein signature. Notice that the work of [27] considered a case in the vicinity of the $\mathcal{PT}$ phase transition, whereas in our setting, such a phase transition is *impossible*, given the real nature of the superpartner Pöschl-Teller potential, as discussed above.

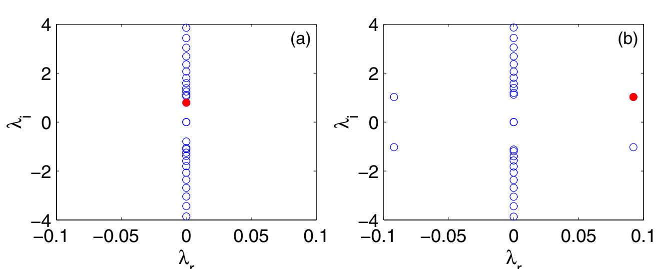

FIG. 6. (Color online) Two case examples of the spectral plane (λ_r,λ_i) of eigenvalues $\lambda = \lambda_r + i\lambda_i$ of the solution for (a) $b_I = 0$ and (b) $b_I = 1$. The eigenvalue which is spectrally stable in the left panel but whose collision with the band edge of the continuous spectrum is responsible for the instability in the right panel is denoted by a red mark.

Figure 5 shows that dipolar solutions with a single node are unstable for almost all of their existence interval except when $2.43 < b_I < 2.5$, i.e., in the immediate vicinity of the linear limit. There are three different instability intervals: (1) for $b_I \leqslant 0.48$ there are two instabilities, one of exponential nature and an oscillatory one; (2) for $0.48 < b_I \leqslant 1.31$ the oscillatory instability is the only one that persists, while the formerly real eigenmode crosses the spectral plane origin and becomes imaginary for larger b_I; and (3) for $1.31 < b_I < 2.43$, there are two oscillatory instabilities, the previously mentioned one, and another one caused (in a way similar to the nodeless case) by its climbing up the imaginary axis of the eigenmode formerly unstable as a real pair, and its eventual collision with an eigenvalue bifurcating from the continuous spectrum.

For nodeless solutions with $\kappa = 3$, we can observe in Figs. 7(a) and 7(b) that the solution is unstable throughout its range of existence because of an eigenmode entering the phonon band and causing oscillatory instabilities; a second localized mode enters at $b_I = 1.33$ and, finally, for $b_I = 1.89$, the soliton becomes exponentially unstable. Analogously, the solutions with a node are unstable for all b_I, incurring, in fact, typically multiple instabilities for each value of the parameter, which can be summarized as follows [see Figs. 7(c) and 7(d)]: an oscillatory instability is present for almost every value of

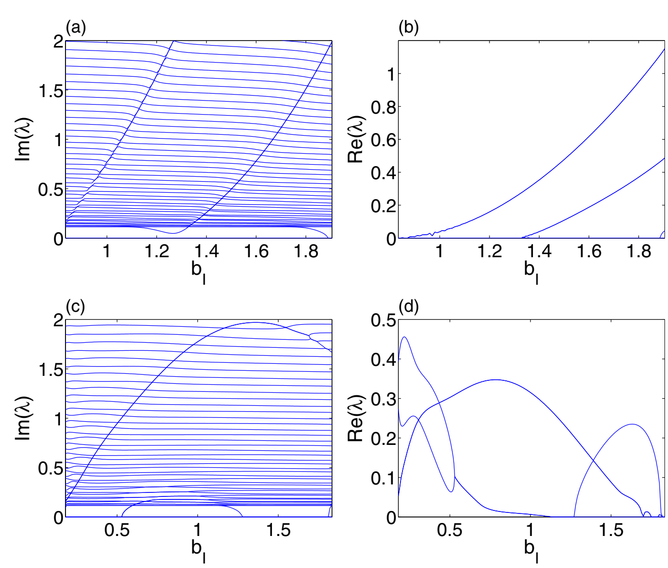

FIG. 7. (Color online) Imaginary part [(a) and (c)] and real part [(b) and (d)] of the eigenvalues associated with the linearization around the solution of the nodeless [(a) and (b)] and the single-node (i.e., dipole) solutions branches [(c) and (d)] for $\kappa = 3$. It can be observed that all the solutions (for different values of b_I) are unstable; see the text for a detailed description of the eigenvalue variation over b_I.

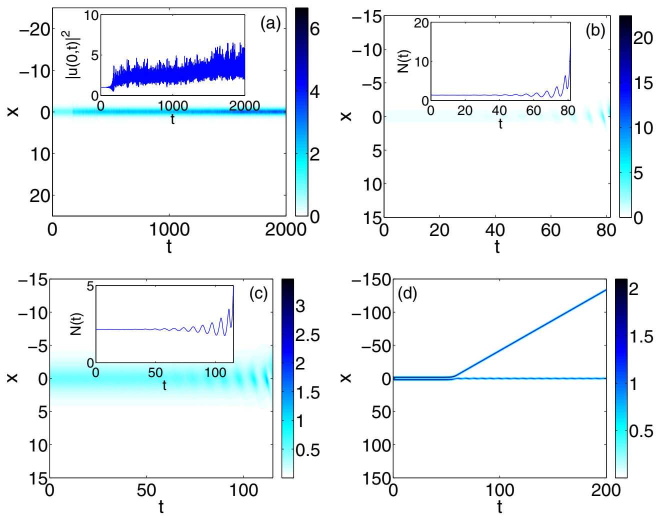

FIG. 8. (Color online) Panel (a): Space-time contour plot of the evolution of the squared modulus (density) of the solution during its unstable dynamics for $b_I = 0.65$ and $\kappa = 1$; the inset shows the evolution of the (maximal) density of the solution occurring at $x = 0$. Panel (b) [(c)] shows the evolution of the density for $b_I = 1$ and $\kappa = 1$ [$\kappa = 3$]; the inset shows the evolution of the norm and displays its eventual indefinite growth. Panel (d) considers the evolution of the unstable soliton with a node for $b_I = 0.2$ and $\kappa = 1$, leading eventually to a split of the two humps into a stationary (at $x = 0$) and a traveling one (at $x < 0$).

b_I ($b_I \lesssim 1.82$); apart from this we observe, for low values of b_I, two pairs of real eigenvalues which coalesce into a quartet at $b_I \approx 0.525$; this quartet leads to two imaginary pairs when $b_I \approx 1.14$; one of them moves down along the imaginary axis and finally, at $b_I \approx 1.27$, an additional instability due to a real pair emerges.

It is relevant to note in passing another interesting result which relates to the $\kappa < 1$ case: we have found that for $\kappa < 2/3$, the nodeless soliton is stable for *every* b_I. This observation and the results above indicate the strong dependence of the stability properties on the precise strength of the nonlinearity parameter.

Finally, we consider the dynamics of these unstable waveforms for several prototypical cases in Fig. 8. For $b_I = 0.65$ and $\kappa = 1$ we observe that when $t \gtrsim 200$, the oscillatory nature (as predicted by our eigenvalue computations) of the instability gradually kicks in and eventually renders the solitary wave more highly localized (i.e., narrower) at $x = 0$ and with a larger amplitude (i.e., taller). Subsequently, the amplitude of the pulse is subject to breathing, but it remains fairly robust, even after multiple collisions with small amplitude radiative wave packets scattering back and forth from the boundaries (not visible at the scale of the plot). For $b_I = 1$ and $\kappa = 1$, the growth rate is larger and the instability effects stronger; it manifests in an oscillatory growth of the soliton (given the oscillatory nature of the instability), as well as a "swinging" of the solution between the gain ($x < 0$) and loss ($x > 0$) regions, according to the terminology of [22]. This eventually leads to rapid growth (beyond the resolution of the numerical scheme). We do not follow the solution past these large values of its amplitude. This behavior is generic for the oscillatory instabilities as long as the growth rate is above a threshold, as shown also in the example for $b_I = 1$ and $\kappa = 3$, and for the nodeless and single-node solitons. Finally, we have considered the effect of the exponential instabilities in solitons with a node and $\kappa = 1$. Those solitons are both exponentially and oscillatorily unstable for $b_I < 0.48$. In that interval, the soliton is double humped (see Fig. 3). In the particular example of Fig. 8, we have taken $b_I = 0.2$ where the exponential instability dominates the oscillatory one. The dynamics here can be described as follows: the hump originally located at the loss ($x > 0$) side shifts and remains pinned with regular oscillations of the amplitude at $x = 0$. On the other hand, the hump initially at the gain ($x < 0$) side is "ejected," as a result of the instability, along the (exponentially localized around $x = 0$) gain side of $x < 0$.

IV. CONCLUSIONS AND FUTURE CHALLENGES

In the present work, we revisited a potential that has been explored previously in a number of studies relating to $\mathcal{PT}$-symmetric models. We discussed how for a special monoparametric family within this model, it is not only $\mathcal{PT}$-symmetric but also supersymmetric with a partner which is the Pöschl-Teller potential, a feature which enabled us to identify its purely real spectrum (and the bifurcations of bound states within it) and to corroborate the corresponding results numerically. As a byproduct of its supersymmetric origin, this family of potentials was found to be devoid of a $\mathcal{PT}$ phase transition. We then turned to a nonlinear variant of the model for arbitrary powers of the nonlinearity and illustrated that exact nonlinear solitonic solutions degenerated in the appropriate limit to the linear states identified previously. While there was no $\mathcal{PT}$ phase transition in this model, we found that the nonlinear solutions were still subject to instabilities, such as the one stemming from a collision of an internal mode with the continuous spectrum (band edge), leading to a quartet of eigenvalues. The ensuing oscillatory instability led to an oscillating, progressively larger amplitude soliton in the cases examined. Additional families of solutions were discussed, including, e.g., the one-node branch (dipolar solution), and their reduced stability (in comparison to the nodeless branch) was illustrated.

While this work, to the best of our understanding, is only a first step in connecting all three notions of $\mathcal{PT}$ symmetry, supersymmetric potentials, and nonlinear phenomenology (including instabilities), naturally this is a theme that is worthy of considerable further studies. For one thing, numerous additional supersymmetric potentials with real spectra can be devised and are worth examining. For instance, the sl$(2,C)$ considerations of [18] already suggest some such options including the superpotentials $W(x) = (m - 1/2)\coth x - ib_I\,\mathrm{cosech}(x)$ or $W(x) = \pm(m - 1/2) - ib_I \exp(\mp x)$. Additionally, there have already been proposals for $\mathcal{PT}$-symmetric square well potentials considered in the SUSY framework [28], and for non-Hermitian SUSY hydrogenlike Hamiltonians with real spectra [29]. Especially in the latter higher dimensional context, understanding the delicate interplay of $\mathcal{PT}$ symmetry, supersymmetric models with their bound states, and collapse induced by nonlinearity could be an especially interesting topic. Finally, there are some potentially intriguing deeper connections. SUSY partners are based on commutation formulas as are integrable nonlinear equations. Perhaps the latter is intrinsically responsible for the similarity of the structure of the SUSY partner potentials with the well-known Miura transformation responsible for converting the modified Korteweg–de Vries equation to the Korteweg–de Vries equation [30]. Although some such connections have already been pointed out [31], exploring these further would constitute an important direction for further studies and efforts along this vein are already underway [32].

ACKNOWLEDGMENTS

This work was supported in part by the US Department of Energy. A.K. wishes to thank the Indian National Science Academy (INSA) for financial support at Pune University. P.G.K. gratefully acknowledges support from NSF-DMS-1312856, the Binational Science Foundation under Grant No. 2010239, and the ERC under FP7, Marie Curie Actions, People, International Research Staff Exchange Scheme (IRSES-605096).

[1] C. M. Bender, Rep. Prog. Phys. **70**, 947 (2007).

[2] See special issues: *Special Issue Dedicated to the Physics of Non-Hermitian Operators* (*PHHQP IV*), edited by H. Geyer, D. Heiss, and M. Znojil, J. Phys. A: Math. Gen. **39**, 9965 (2006); *Papers Dedicated to the Subject of the 6th International Workshop on Pseudo-Hermitian Hamiltonians in Quantum Physics* (*PHHQPVI*), edited by A. Fring, H. Jones, and M. Znojil, J. Phys. A: Math. Theor. **41**, 240301 (2008); *Special Issue: Quantum Physics with Non-Hermitian Operators*, edited by C. M. Bender, A. Fring, U. Günther, and H. Jones, *ibid.* **45**, 440301 (2012).

[3] K. G. Makris, R. El-Ganainy, D. N. Christodoulides, and Z. H. Musslimani, Int. J. Theor. Phys. **50**, 1019 (2011).

[4] A. Ruschhaupt, F. Delgado, and J. G. Muga, J. Phys. A: Math. Gen. **38**, L171 (2005).

[5] K. G. Makris, R. El-Ganainy, D. N. Christodoulides, and Z. H. Musslimani, Phys. Rev. Lett. **100**, 103904 (2008); S. Klaiman, U. Günther, and N. Moiseyev, *ibid.* **101**, 080402 (2008); O. Bendix, R. Fleischmann, T. Kottos, and B. Shapiro, *ibid.* **103**, 030402 (2009); S. Longhi, *ibid.* **103**, 123601 (2009); Phys. Rev. B **80**, 235102 (2009); Phys. Rev. A **81**, 022102 (2010).

[6] A. Guo, G. J. Salamo, D. Duchesne, R. Morandotti, M. Volatier-Ravat, V. Aimez, G. A. Siviloglou, and D. N. Christodoulides, Phys. Rev. Lett. **103**, 093902 (2009); C. E. Rüter, K. G. Makris, R. El-Ganainy, D. N. Christodoulides, M. Segev, and D. Kip, Nat. Phys. **6**, 192 (2010); A. Regensburger, C. Bersch, M.-A. Miri, G. Onishchukov, D. N. Christodoulides, and U. Peschel, Nature **488**, 167 (2012).

[7] J. Schindler, A. Li, M. C. Zheng, F. M. Ellis, and T. Kottos, Phys. Rev. A **84**, 040101 (2011).

[8] J. Schindler, Z. Lin, J. M. Lee, H. Ramezani, F. M. Ellis, and T. Kottos, J. Phys. A: Math. Theor. **45**, 444029 (2012).

[9] C. M. Bender, B. Berntson, D. Parker, and E. Samuel, Am. J. Phys. **81**, 173 (2013).

[10] B. Peng, S. K. Özdemir, F. Lei, F. Monifi, M. Gianfreda, G. L. Long, S. Fan, F. Nori, C. M. Bender, and L. Yang, Nature Physics **10**, 394 (2014).

[11] F. Cooper, A. Khare, and U. Sukhatme, *Supersymmetry in Quantum Mechanics* (World Scientific, Singapore, 2002).

[12] M.-A. Miri, M. Heinrich, R. El-Ganainy, and D. N. Christodoulides, Phys. Rev. Lett. **110**, 233902 (2013); M. Heinrich, M. A. Miri, S. Stützer, R. El-Ganainy, S. Nolte, A. Szameit, and D. N. Christodoulides, Nat. Comm. **5**, 3698 (2014).

[13] M.-A. Miri, M. Heinrich, and D. N. Christodoulides, Phys. Rev. A **87**, 043819 (2013).

[14] Z. Lin, H. Ramezani, T. Eichelkraut, T. Kottos, H. Cao, and D. Christodoulides, Phys. Rev. Lett. **106**, 213901 (2011).

[15] B. Midya, Phys. Rev. A **89**, 032116 (2014).

[16] G. Poschl and E. Teller, Z. Phys. **83**, 143 (1933).

[17] L. D. Landau and E. M. Lifshitz, *Quantum Mechanics* (Nauka, Moscow, 1989).

[18] B. Bagchi, S. Mallik, and C. Quesne, Int. J. Mod. Phys. A **16**, 2859 (2001).

[19] B. Bagchi and R. Roychoudhury, J. Phys. A **33**, L1 (2000).

[20] Z. Ahmed, Phys. Lett. A **282**, 343 (2001).

[21] Z. H. Musslimani, K. G. Makris, R. El-Ganainy, and D. N. Christodoulides, Phys. Rev. Lett. **100**, 030402 (2008).

[22] M. Nazari, F. Nazari, and M. K. Moravvej-Farshi, J. Opt. Soc. Am. B **29**, 3057 (2012).

[23] H. Chen, S. Hu, and L. Qi, Opt. Commun. **331**, 139 (2014).

[24] B. Bagchi and C. Quesne, Phys. Lett. A **273**, 285 (2000).

[25] A. S. Reyna and C. B. de Araújo, Phys. Rev. A **89**, 063803 (2014); A. S. Reyna, K. C. Jorge, and C. B. de Araújo, *ibid.* **90**, 063835 (2014).

[26] T. Kapitula, P. G. Kevrekidis, and B. Sandstede, Physica D **195**, 263 (2004).

[27] S. Nixon and J. Yang, arXiv:1506.04445.

[28] B. Bagchi, S. Mallik, and C. Quesne, Mod. Phys. Lett. A **17**, 1651 (2002).

[29] O. Rosas-Ortiz and R. Muñoz, J. Phys. A **36**, 8497 (2003).

[30] P. G. Drazin and R. S. Johnson, *Solitons: An Introduction* (Cambridge University, Cambridge, England, 1989).

[31] M. Wadati, J. Phys. Soc. Jpn. **77**, 074005 (2008).

[32] A. Koller and M. Olshanii, Phys. Rev. E **84**, 066601 (2011).